

AB-INITIO PULSAR MAGNETOSPHERE: THREE-DIMENSIONAL PARTICLE-IN-CELL SIMULATIONS OF OBLIQUE PULSARS.

ALEXANDER A. PHILIPPOV¹, ANATOLY SPITKOVSKY & BENOIT CERUTTI
Department of Astrophysical Sciences, Princeton University, Ivy Lane, Princeton, NJ 08540
Draft version December 3, 2014

ABSTRACT

We present “first-principles” relativistic particle-in-cell simulations of the oblique pulsar magnetosphere with pair formation. The magnetosphere starts to form with particles extracted from the surface of the neutron star. These particles are accelerated by surface electric fields and emit photons capable of producing electron-positron pairs. We inject secondary pairs at locations of primary energetic particles, whose energy exceeds the threshold for pair formation. We find solutions that are close to the ideal force-free magnetosphere, with the Y-point and current sheet. Solutions with obliquities $\leq 40^\circ$ do not show pair production in the open field line region, because the local current density along magnetic field is below the Goldreich-Julian value. The bulk outflow in these solutions is charge separated, and pair formation happens in the current sheet and return current layer only. Solutions with higher inclinations show pair production in the open field line region, with high multiplicity of the bulk flow and the size of pair-producing region increasing with inclination. We observe the spin-down of the star to be comparable to MHD model predictions. The magnetic dissipation in the current sheet ranges between 20% for the aligned rotator and 3% for the orthogonal rotator. Our results suggest that for low obliquity neutron stars with suppressed pair formation at the light cylinder, the presence of phenomena related to pair activity in the bulk of the polar region, e.g., radio emission, may crucially depend on the physics beyond our simplified model, such as the effects of curved space-time or multipolar surface fields.

Subject headings: plasmas – pulsars: general – stars: magnetic field – stars: rotation

1. INTRODUCTION

In the last 15 years the pulsar magnetosphere was intensively studied in the magnetohydrodynamic (MHD) limit, including ideal force-free electrodynamic (Contopoulos et al. 1999; Gruzinov 2005; McKinney 2006; Timokhin 2006; Spitkovsky 2006; Kalapotharakos & Contopoulos 2009; Pétri 2012), resistive force-free (Li et al. 2012; Kalapotharakos et al. 2012), and full relativistic MHD (Komissarov 2006; Tchekhovskoy et al. 2013). While these solutions agree on the general shape of the plasma-filled magnetosphere, the origin of the magnetospheric plasma and the properties of particle acceleration necessary for production of observed radiation cannot be addressed within the MHD approach, necessitating a kinetic treatment.

Recently, the aligned pulsar magnetosphere was studied with first-principles relativistic particle-in-cell simulations (Philippov & Spitkovsky 2014, hereafter, PS14; Chen & Beloborodov 2014, hereafter, CB14; Cerutti et al. 2014). PS14 showed that injecting abundant pairs everywhere in the magnetosphere drives the solution towards the force-free configuration. Cerutti et al. (2014) studied the transition between the disk-dome configuration and the filled solution by varying the rate of particle injection at the stellar surface. Beloborodov (2008) and Timokhin & Arons (2013) studied one-dimensional polar cap cascade and found that in the region where current density along the magnetic field, j_{\parallel} , is below the Goldreich-Julian value, $j_{GJ} = -\Omega_* \cdot \mathbf{B}/2\pi$ (here, Ω_* is the stellar angular velocity vector, and \mathbf{B} is the local

magnetic field), particles in the space-charge-limited flow are not accelerated up to relativistic energies and do not produce secondary pairs. Efficient particle acceleration, and, consequently, active pair formation, should thus be confined to the regions where $j_{\parallel}/j_{GJ} < 0$ or $j_{\parallel}/j_{GJ} > 1$. CB14 presented the first global aligned simulation with e^{\pm} discharges and concluded that pair formation in the outer magnetosphere is required to produce the solution similar to force-free but with strong charge separation, consistent with sub-GJ current flow in the polar cap region. This raised the question of whether high-multiplicity state of the magnetosphere is ever achieved, particularly in more realistic oblique rotators.

The goal of this Letter, therefore, is to describe the magnetospheres of oblique pulsars. For this, we construct relativistic particle-in-cell (PIC) simulations of the oblique pulsar with different prescriptions for populating the magnetosphere with plasma, focusing on solutions with realistic prescription for pair formation. The Letter is organized as follows. In §2 we describe our numerical method, in §3 we demonstrate the test solution with abundant neutral plasma supply, and in §4 we present our results on three-dimensional magnetosphere structure of aligned and oblique rotators with pair production.

2. NUMERICAL METHOD AND SETUP

To simulate the magnetosphere we use the 3D electromagnetic PIC code TRISTAN-MP (Spitkovsky 2005). To a good accuracy, the star can be described as a rotating magnetized conductor. Unipolar induction generates electric fields corresponding to a quadrupolar surface charge. In the limit of zero work function these charges can be pulled from the surface by the electric field, popu-

¹ sashaph@princeton.edu

lating the magnetosphere with plasma. Below we ignore the complications of extracting ions from the surface and assume that extracted positive charges are positrons. In addition to extraction of surface charges, we consider two scenarios for plasma supply. First, we extend the study of PS14 to oblique rotators by considering abundant neutral plasma injection in the whole magnetosphere. Second, we add a more realistic prescription, which approximates pair production by magnetic conversion of photons and two-photon collisions (see §4.1).

We use linearity of Maxwell’s equations to represent the electric field as a superposition: $\mathbf{E} = \mathbf{E}_{\text{vacuum}} + \mathbf{E}_{\text{plasma}}$, where $\mathbf{E}_{\text{vacuum}}$ is the analytical field of the vacuum rotator (Michel & Li 1999), and $\mathbf{E}_{\text{plasma}}$ is the field computed from PIC particles (Spitkovsky & Arons 2002). The same decomposition is done for the magnetic field. Inside the conducting sphere, the plasma fields are forced to zero with a smoothing kernel, while the vacuum fields are set to corotation values.

We use a Cartesian grid of 1024^3 cells, with stellar radius $R_* = 35$ cells, and light cylinder $R_{LC} = 120$ cells. Particles penetrating into the star by two cells are removed. The outer walls have radiation boundary conditions for fields and particles.

3. TEST PROBLEM: “FORCE-FREE” SOLUTION

In this section we extend PS14 and build a force-free solution for the oblique rotator. Neutral pair plasma is injected with zero velocity at a fixed rate in every cell within a sphere of $R = 2R_{LC}$, if the magnetization in a cell exceeds a certain limit, $\sigma = B^2/(4\pi nm_e c^2) > 1000(R_*/r)^3$. Here, B is the absolute value of the magnetic field, and n is the plasma density. This limiter helps to prevent overloading of the magnetosphere with plasma, particularly in the closed zone, while keeping the flow well-magnetized. The magnetization of our solution is $\sigma \approx 1000$ near the pole (around 20 particles per cell, local skin depth is 1.1 cells), and $\sigma \approx 20$ at the light cylinder (around 1 particle per cell, local skin depth is 5 cells).

Magnetic field in the plane defined by the magnetic moment $\boldsymbol{\mu}$ and stellar angular velocity $\boldsymbol{\Omega}_*$ vectors for 60° rotator is shown in Fig. 1c, where color represents the out-of-plane component of the magnetic field. In agreement with the MHD solution (Tchekhovskoy et al. 2013), poloidal field lines in this plane become purely radial beyond R_{LC} . The Y-point is located approximately at the light cylinder, and the current sheet oscillates around the equatorial plane. As shown in Fig. 1a,b, our kinetic solution has high multiplicity (≈ 10) in the bulk of the polar outflow, which carries sub-GJ current (see Fig. 1d). The regions with current above the GJ value, favorable for efficient pair formation, are the current sheet and the rims of the polar cap, where volume return current flows².

The field structure is quasi-stable in the corotating frame. We note that within the simulation box the role of drift-kink instability of the current sheet, pointed out for the aligned rotator by PS14 and studied by Cerutti et al. (2014), decreases with increasing obliquity, becoming negligible already for 60° . This is a consequence of

the decrease of conduction current in the current sheet with increasing obliquity.

We ran simulations for obliquities 30° , 60° and 90° , measuring the Poynting flux integrated over a sphere with $r = R_{LC}$. Combining with the aligned case (PS14), we conclude that the spin-down energy loss of the PIC solution is consistent with MHD studies:

$$L = \frac{\mu^2 \Omega_*^4}{c^3} (k_0 + k_1 \sin^2 \chi), \quad (1)$$

with coefficients $k_0 = 1.0 \pm 0.1$, $k_1 = 1.1 \pm 0.1$ (see Figure 5), and χ the inclination angle.

4. PULSAR MAGNETOSPHERE

4.1. Pair creation process

In order to mimic the surface charge injection, we inject neutral plasma everywhere on the star with a rate of $0.2\Sigma = 0.2(E_r(r_*) - E_r^{cor}(r_*))/4\pi$ per time step, where Σ is the local surface charge, r_* is the injection point at the stellar surface, and E_r^{cor} is the r -component of the corotation electric field. We found that, in general, E_{\parallel} is not effectively screened at the surface for lower injection rates, while larger rates lead to virtual cathode oscillations. Even though we inject neutral plasma, the particles are injected at rest, and one sign of charge is pulled into the star, while the other is accelerated into the magnetosphere.

In real pulsars, the particles that are accelerated above the polar cap emit high-energy curvature photons that produce pairs via magnetic conversion. The pairs are created in non-zero Landau levels and emit synchrotron radiation that might also be converted into pairs. In addition to magnetic conversion of photons, the electron-positron pairs may be produced in $\gamma - \gamma$ collisions. In this study we ignore the mean free path of photons and produce secondary pairs at the location of primary energetic particles, whenever the energy of a particle exceeds the threshold $\gamma > \gamma_{min}$. The threshold value is set to $\gamma_{min} = 0.02\gamma_0 = 40$, where γ_0 is the full vacuum potential drop between the pole and the equator, $\gamma_0 = (\Omega_* R_*/c)(B_0 R_*/c^2) \approx 2000$. The threshold does not depend on the distance from the star. The rate of pair creation per particle in our simulation is $2\gamma/\gamma_{min}$ per time step. These simulation parameters help ensure sufficient pair supply in the regions of magnetosphere where pair production is possible. In reality, in addition to particle energy, the threshold and pair yield of both the magnetic conversion and $\gamma - \gamma$ collisions depend on the strength and curvature of the local magnetic field. Our aim is not to model the true multiplicity of the flow, but to identify the regions of active pair formation that can yield high multiplicity. By using a pair production prescription that does not depend on the local magnetic field, we obtain an upper limit on the number of such active regions. In order to resolve the skin depth and minimize computational cost, we put a limiter on the number of produced pairs, so that multiplicity in every cell where pairs are produced does not exceed 10. The secondary pairs are injected in the direction of primary particle motion, and are randomly distributed in the computational cell of the parent. Their Lorentz factor is set to 4, much less than that of the parent particle. We subtract the energy of produced pairs from the energy of the parent

² The pair producing rim is located at the southern part of the polar cap (for the northern hemisphere), unrelated to the location of “favorably curved” field lines (Arons & Scharlemann 1979).

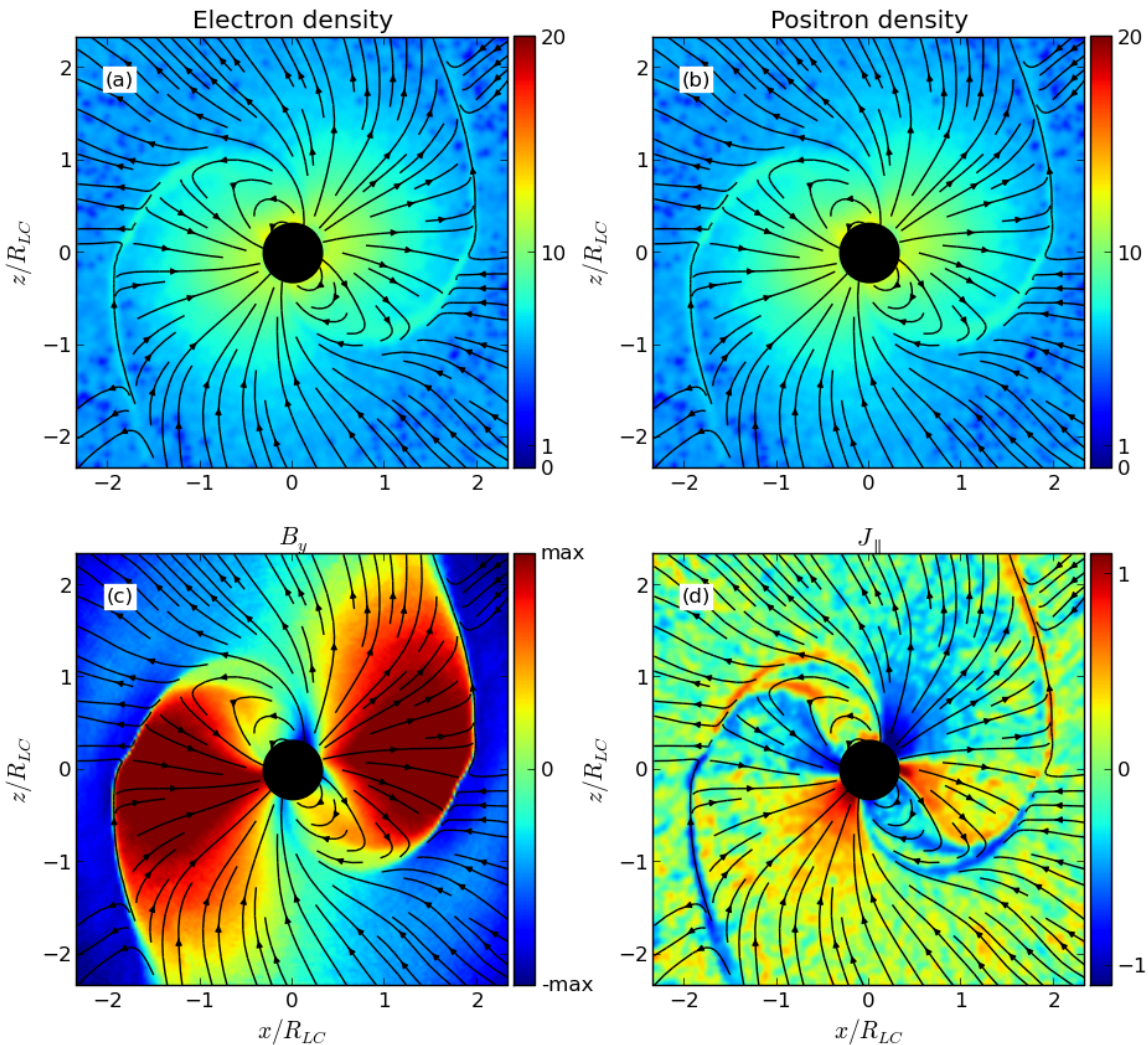


FIG. 1.— Slice through the $\mu - \Omega_*$ plane for $\chi = 60^\circ$ pulsar magnetosphere with abundant pair injection, shown after two rotational periods, $R_*/R_{LC} = 0.3$: (a, b) electron and positron density distribution, normalized by $\Omega_* B/2\pi ec$; poloidal field lines are shown in black; (c) out-of-plane component of the magnetic field (color); (d) current component parallel to the magnetic field, normalized by $\Omega_* B/2\pi$.

particle, accounting for the effect of radiation reaction force.

4.2. Aligned rotator

The magnetosphere of the aligned rotator with self-consistent pair formation is shown in Fig. 2c. Its magnetic field structure is close to the force-free solution: field becomes mostly toroidal beyond R_{LC} , and poloidal field lines stretch and become radial. The opposite polarities of toroidal field are supported by the equatorial current sheet. We observe moderate kinking of the sheet beyond $2R_{LC}$, that does not affect the Y-point region during our simulation.

The polar region is inactive to pair formation, as pointed out by Timokhin & Arons (2013) and CB14. This happens because the current flow is sub-GJ (see Figure 2d), thus E_{\parallel} within the light cylinder is easily screened by sub-relativistic electron outflow shown in

Figure 2a. However, pair production does take place in the return current layer and in the current sheet, which have high multiplicity of secondary pairs as shown in Fig. 2a,b. The acceleration of parent particles occurs due to strong E_{\parallel} in the current sheet. The electric field points away from the star, and positrons are accelerated outwards, while high-energy electrons stream towards the star. These electrons pass through the Y-point and penetrate into the inner magnetosphere by a few Larmor radii. The current sheet width scales with magnetic field strength at the light cylinder, staying of the order of average Larmor radius of particles. Most of the open field lines do not cross the null surface, and the electron outflow on these lines extends to infinity. The last open field lines, however, go through the null surface. Since the electron outflow cannot cross the null surface, a vacuum gap opens above the current sheet (cf. CB14). The spin-down of this solution, measured as the flux of electro-

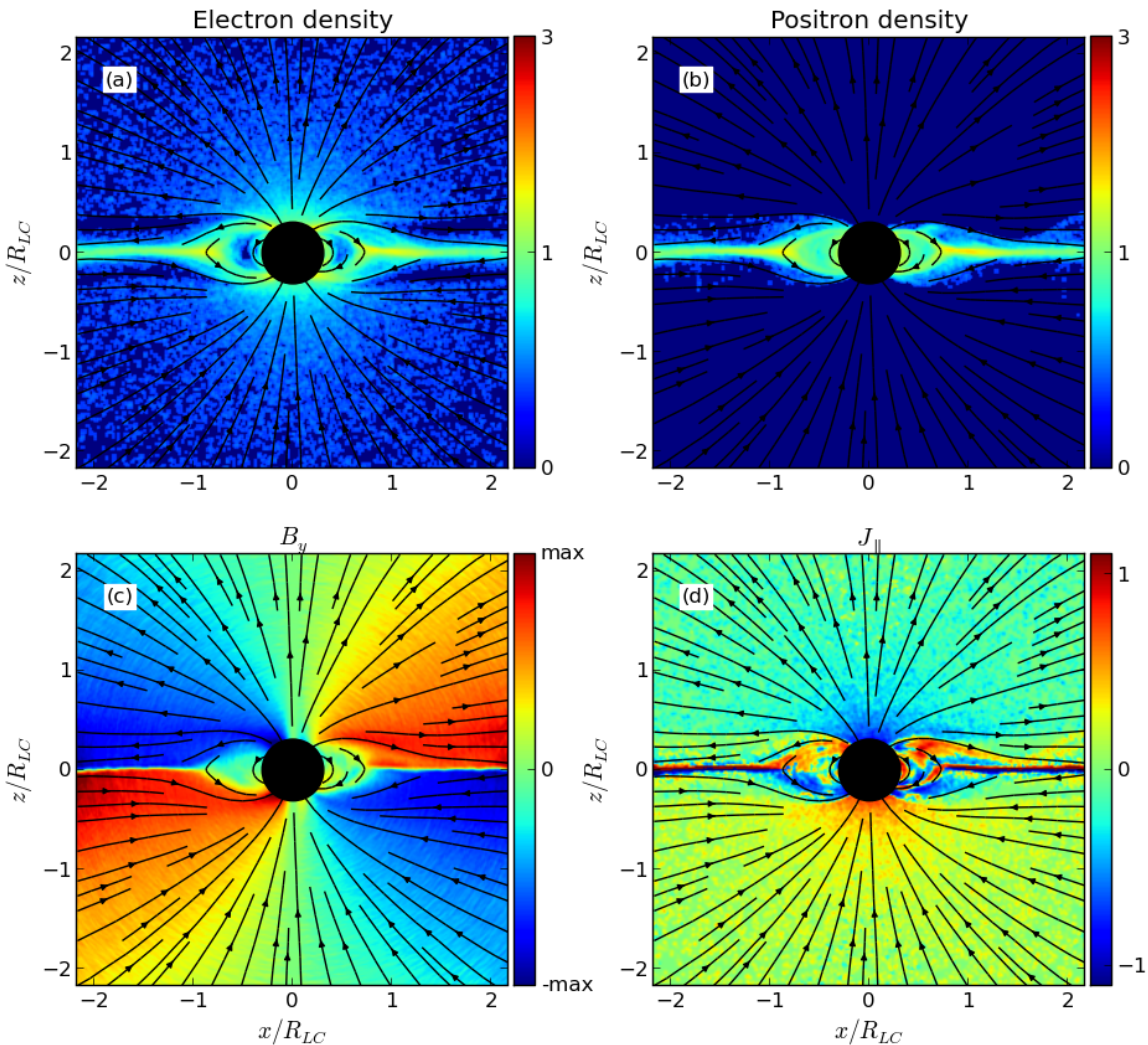


FIG. 2.— Same as Fig. 1, but for aligned pulsar magnetosphere with self-consistent pair formation.

magnetic energy at the stellar surface, is $\approx 0.85\mu^2\Omega_*^4/c^3$.

We note that confining pair creation to inner magnetosphere, $r \leq 2R_*$, or increasing the global pair creation threshold to values comparable with $\gamma \approx \sigma_{LC}$, where σ_{LC} is the magnetization parameter at the light cylinder, leads to the suppression of return current, and the magnetosphere relaxes to the low multiplicity solution (Cerutti et al. 2014; CB14). In this state the magnetosphere consists of an equatorial disk of positrons and a polar dome of electrons. Positrons are pulled from the tip of the disk by strong electric field, $E > B$; however, the resulting current is not large enough to substantially modify the dipolar magnetic field structure.

4.3. Oblique rotator

We found that magnetospheres of rotators with inclination angles $\chi \lesssim 40^\circ$ are qualitatively similar to the aligned solution, showing no pair creation activity in the polar cap outflow. The bulk outflow in these solutions is charge-separated, and pair production happens only in

the current sheet and the return layer. These solutions relax to the oblique disk-dome structure if the pair production in the outer magnetosphere is suppressed. This happens because the return current layer, where pair production is possible, cannot be formed by particles lifted from the surface, since the sign of the necessary current is opposite to the sign of available charges. As there is no current outflow, the oblique disk-dome solutions spin down at the vacuum rate.

Solutions with high obliquities, $\chi \gtrsim 40^\circ$, do show pair creation in the polar cap zone. There are regions on the polar cap with volume return current exceeding the GJ value (Timokhin & Arons 2013). The structure of the 60° rotator is shown in Figure 3c. The magnetospheric structure is similar to what we found in §3, with closed and open zones, Y-point and the current sheet. Pairs are produced in the region of volume return current and in the current sheet. The flow in the sheet is supported not only by the local pair creation, as in the case of the aligned rotator, but also by the reconnection-

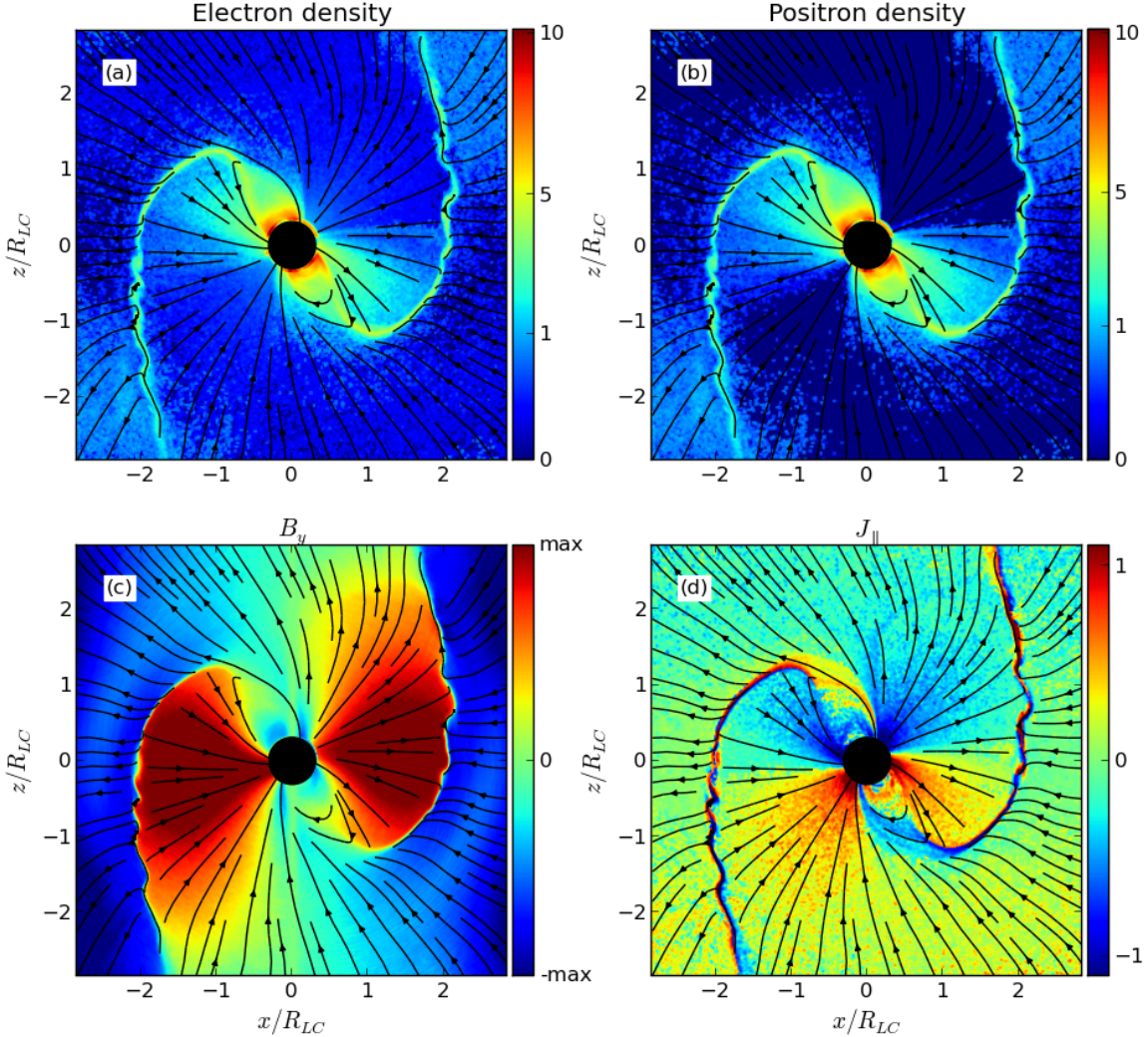


FIG. 3.— Same as Fig. 1, but for $\chi = 60^\circ$ pulsar magnetosphere with self-consistent pair formation.

induced inflow of charges produced in the polar cap discharge. The plasma density is not uniform in the polar cap as seen from Figures 3a and b. Part of the polar cap supports charge-separated electron outflow with $\alpha = j_{\parallel}/j_{GJ} \approx 0.95 < 1$. The Lorentz factor of this flow is ≈ 25 , independent of the surface magnetic field. This is consistent with the estimate $\gamma \approx 2\alpha/(1 - \alpha^2)$ for the space-charge-limited flow (Beloborodov 2008; Timokhin & Arons 2013) in the case of sub-GJ current. The volume return current region shows active pair production. The polar discharge has quasi-periodic behavior on the timescales short compared to the pulsar rotation period, with episodes of efficient pair production followed by quiet states. The three-dimensional study of the cascade intermittency is important for modelling the pulsar radio emission and will be discussed elsewhere. The multiplicity of the flow in the active region of the polar cap is ≈ 10 , close to the limiting value. We performed a simulation with twice larger limiting value and observed that the multiplicity of the flow increases by roughly the

same factor. Though not the whole polar cap shows active pair formation, on average the pulsar wind is supplied with plasma of high multiplicity, concentrated in the equatorial current sheet wedge. The current sheet beyond the light cylinder should thus be the main source of γ -photons, and the polar cap discharge is a candidate for the “bridge” emission. As in the aligned case, mainly positrons are accelerated in the current sheet of the 60° rotator. We find that current sheet of the pair forming solution shows more efficient kinking than the test solution from §4, though it does not strongly affect the global magnetospheric structure.

We find that the volume return current region in our simulations is bounded by the null surface that crosses the polar cap; this current is carried by positrons. However, in the limit of very small star $R_*/R_{LC} \rightarrow 0$ the null surface is located outside the polar cap for inclinations that are not too close to 90° , and the outflowing current is supposed to be carried only by electrons. Thus,

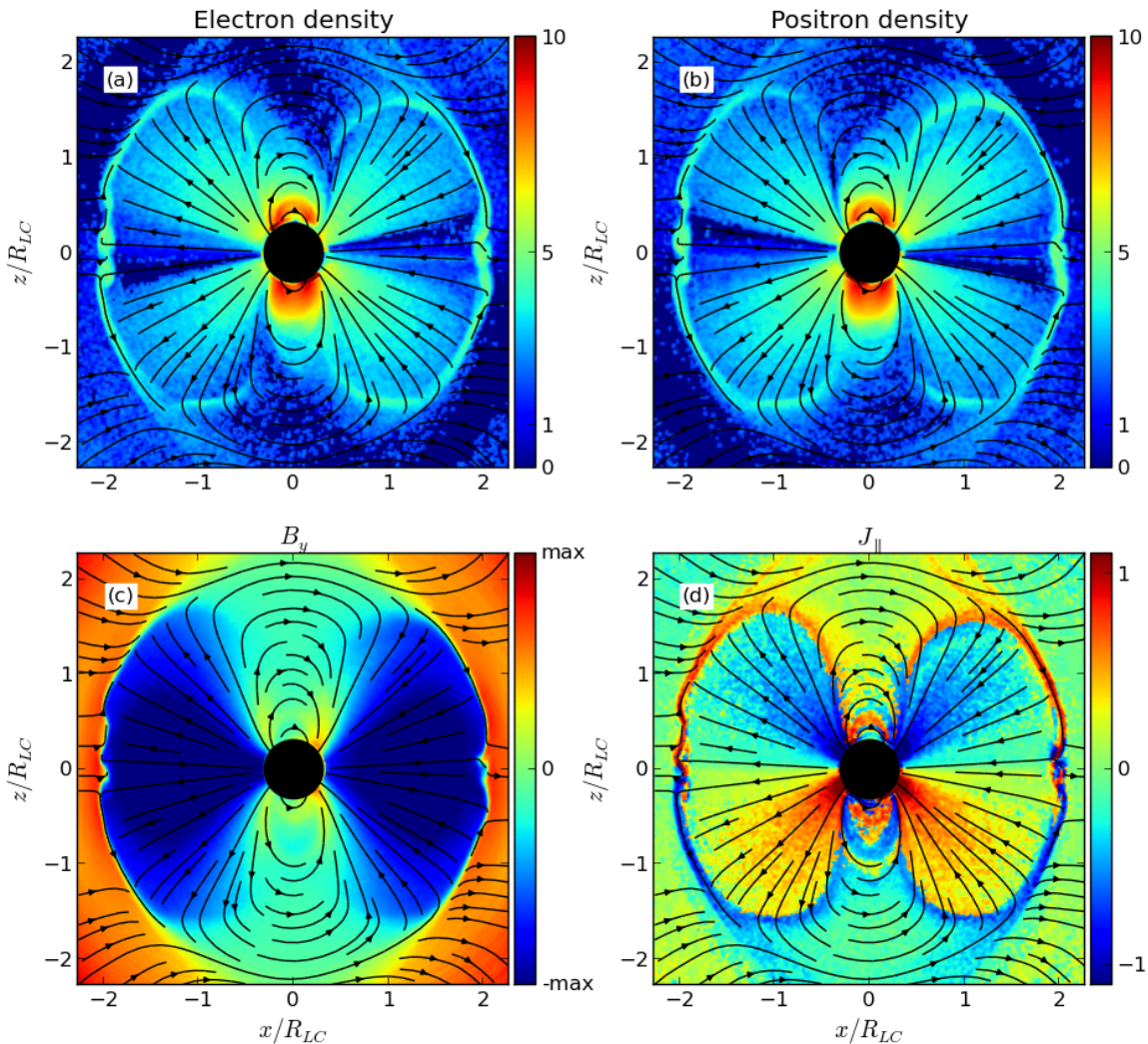


FIG. 4.— Same as Fig. 1, but for orthogonal pulsar magnetosphere with self-consistent pair formation.

the pair-producing region with $j > j_{GJ}$ may disappear³. We conclude that precise obliquity angle for transition between active and inactive state of the polar cap may change for $R_* \ll R_{LC}$. Although our present simulations are already physically relevant for millisecond pulsars with high R_*/R_{LC} , we will investigate the smaller values of R_*/R_{LC} in future work.

The 90° rotator shows efficient pair production in the whole polar cap (Fig. 4). In contrast to the aligned rotator, the current flow on the polar cap is anti-symmetric with respect to the equatorial plane. Current density exceeds j_{GJ} , necessitating the presence of e^\pm discharge. Pair formation also happens in the current sheet. Moderate kinking of the sheet is observed close to the equatorial plane.

In Figure 5 we present the spin-down of our oblique solutions with pair formation, measured at the stellar

³ However, the value of $j_{||}/j_{GJ}$ in the bulk region for the small stellar radius may also change.

surface. In our solution for the aligned rotator with pair discharges approximately 20% of the Poynting flux is dissipated within $2R_{LC}$. The dissipated fraction of total energy losses decreases for larger inclination angles and reaches 3% for the orthogonal rotator. The dissipated energy is converted into particle energy in acceleration regions. The deviation of spin-down from solutions with abundant pair formation discussed in §3 is small and becomes negligible with increasing inclination. The origin of this deviation is due to the presence of vacuum-like regions inside the light cylinder that are not in corotation with the star.

5. DISCUSSION

In this Letter we presented the magnetospheric structure of oblique pulsars with pair formation. We found that pulsars with low obliquities produce active solutions only if pair formation in the outer magnetosphere is working. In these solutions the pairs are produced in the equatorial current sheet beyond the light cylinder and

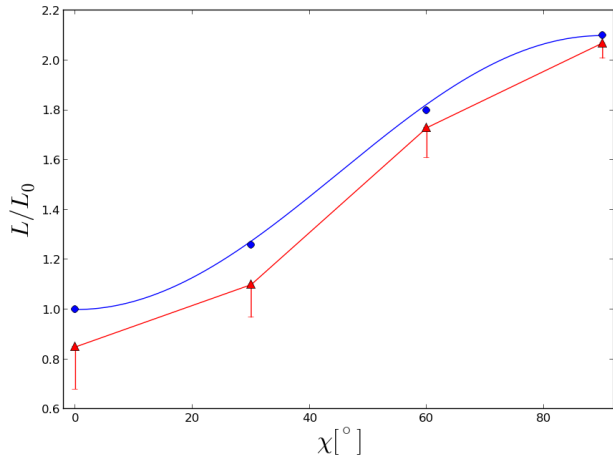


FIG. 5.— Poynting flux luminosity of solutions with realistic pair formation in units of $L_0 = \mu^2 \Omega_*^4 / c^3$ as a function of the inclination angle (red triangles), measured at the stellar surface. The error bars correspond to the dissipated fraction of the Poynting flux within $2R_{LC}$. Blue points show the results of PIC simulations with abundant pair formation (§3), and the blue curve shows prediction of the MHD model.

in the return current layer. If the radio emission is produced in the high multiplicity flow at the polar cap, these pulsars should have mainly double-peaked profiles associated with return current layers. Pulsars with obliquity angles $\gtrsim 40^\circ$ show significant pair production activity in the polar regions. Their radio beams may have multi-peaked structure. The spin-down of pair solutions is close to MHD model predictions.

Our prescription for pair formation is highly idealized. For simplicity we neglected the mean free path of photons and assumed the pair formation threshold to be independent of the local conditions. While this approximation is reliable for the polar cap discharge, the $\gamma - \gamma$ process which can account for the activity in the current sheet is intrinsically non-local, which requires more careful treatment. Two processes may contribute to launching the e^\pm discharge in the current sheet: collisions of energetic synchrotron photons emitted by counter-streaming particle flows, and collisions of thermal X-ray photons from

the neutron star surface, which may be up-scattered by energetic particles in the sheet, with synchrotron photons. Both mechanisms should operate most efficiently close to the Y-point, where magnetic field in the sheet is strongest, and the emitted synchrotron photons are the most energetic. We assumed efficient pair formation in the current sheet, which may not happen in pulsars with low magnetic field strength at the light cylinder. In low obliquity pulsars with no pair formation in the current sheet, the return current layer is suppressed, and such pulsars should not shine in the radio band, unless some physics beyond our model can reestablish pair formation.

A potentially important complication may arise due to the restricted ability of ions to produce pairs. Though ions can still emit curvature photons capable of producing pairs in $\gamma - \gamma$ collisions with stellar photons, the resulting multiplicity of the flow due to this process is uncertain. This may affect the multiplicity of the polar outflow in the orthogonal rotator, where ions are extracted in the half of the polar cap.

The poloidal field at the stellar surface may be more complicated than the pure dipole field considered in this work due to the operation of Hall effect in the crust (e.g., Gourgouliatos & Cumming 2014). The resulting multipolar field can modify the operation of the polar discharge, producing more regions with efficient pair production.

The value of $\alpha = j_{\parallel} / j_{GJ}$ that is essential for operation of polar discharge may be sensitive to general relativistic corrections. In particular, the value of GJ charge density is reduced due to Lense-Thirring effect (Beskin 1990; Muslimov & Tsygan 1992). The increased value of α may lead to the ignition of polar discharge in low obliquity pulsars. This will be investigated in future work.

We thank Jonathan Arons, Vasily Beskin, Alexander Tchekhovskoy, and Andrey Timokhin for fruitful discussions. This research was supported by NASA grants NNX12AD01G and NNX13AO80G, Simons Foundation (grant 267233 to AS), and was facilitated by Max Planck/Princeton Center for Plasma Physics. The simulations presented in this article used computational resources supported by the PICSciE-OIT High Performance Computing Center and Visualization Laboratory.

REFERENCES

- Arons, J., & Scharlemann, E. T. 1979, *ApJ*, 231, 854
 Beloborodov, A. M. 2008, *ApJ*, 683, L41
 Beskin, V. S. 1990, *Soviet Astronomy Letters*, 16, 286
 Cerutti, B., Philippov, A., Parfrey, K., & Spitkovsky, A. 2014, ArXiv e-prints, arXiv:1410.3757
 Chen, A. Y., & Beloborodov, A. M. 2014, *ApJ*, 795, L22
 Contopoulos, I., Kazanas, D., & Fendt, C. 1999, *ApJ*, 511, 351
 Gourgouliatos, K. N., & Cumming, A. 2014, *MNRAS*, 438, 1618
 Gruzinov, A. 2005, *Physical Review Letters*, 94, 021101
 Kalapotharakos, C., & Contopoulos, I. 2009, *A&A*, 496, 495
 Kalapotharakos, C., Contopoulos, I., & Kazanas, D. 2012, *MNRAS*, 420, 2793
 Komissarov, S. S. 2006, *MNRAS*, 367, 19
 Li, J., Spitkovsky, A., & Tchekhovskoy, A. 2012, *ApJ*, 746, 60
 McKinney, J. C. 2006, *MNRAS*, 368, L30
 Michel, F. C., & Li, H. 1999, *Phys. Rep.*, 318, 227
 Muslimov, A. G., & Tsygan, A. I. 1992, *MNRAS*, 255, 61
 Pétri, J. 2012, *MNRAS*, 424, 605
 Philippov, A. A., & Spitkovsky, A. 2014, *ApJ*, 785, L33
 Spitkovsky, A. 2005, in *AIP Conf. Ser.*, Vol. 801, *Astrophysical Sources of High Energy Particles and Radiation*, ed. T. Bulik, B. Rudak, & G. Madejski, 345
 Spitkovsky, A. 2006, *ApJ*, 648, L51
 Spitkovsky, A., & Arons, J. 2002, in *ASP Conf. Ser.*, Vol. 271, *Neutron Stars in Supernova Remnants*, ed. P. O. Slane & B. M. Gaensler, 81
 Tchekhovskoy, A., Spitkovsky, A., & Li, J. G. 2013, *MNRAS*, 435, L1
 Timokhin, A. N. 2006, *MNRAS*, 368, 1055
 Timokhin, A. N., & Arons, J. 2013, *MNRAS*, 429, 20